Note: A phase synchronization photography method for AC discharge

Zhicheng Wu, Qiaogen Zhang, Jingtan Ma, and Lei Pang

Citation: Review of Scientific Instruments **89**, 056107 (2018); doi: 10.1063/1.5031080
View online: https://doi.org/10.1063/1.5031080
View Table of Contents: http://aip.scitation.org/toc/rsi/89/5
Published by the American Institute of Physics

Note: A phase synchronization photography method for AC discharge

Zhicheng Wu, Qiaogen Zhang, Jingtan Ma, and Lei Pang[a)]
State Key Laboratory of Electrical Insulation and Power Equipment, Xi'an Jiaotong University, Xi'an 710049, China

(Received 28 March 2018; accepted 2 May 2018; published online 30 May 2018)

To research discharge physics under AC voltage, a phase synchronization photography method is presented. By using a permanent-magnet synchronous motor to drive a photography mask synchronized with a discharge power supply, discharge images in a specific phase window can be recorded. Some examples of discharges photographed by this method, including the corona discharge in SF_6 and the corona discharge along the air/epoxy surface, demonstrate the feasibility of this method. Therefore, this method provides an effective tool for discharge physics researchers. *Published by AIP Publishing.*
https://doi.org/10.1063/1.5031080

Power system engineers and plasma scientists are interested in the AC voltage discharge. For instance, the condition monitoring of overhead lines and gas-insulated metal-enclosed switchgears are closely related to gas discharge physics.[1,2] In the field of chemical environmental protection, dielectric barrier discharges in AC voltage are applied to exhaust gas processing.[3]

The imaging diagnosis of the discharge at different time scales is an important tool for researchers who study the spatial resolution of plasma. Since the discharge occurs mainly at the nanosecond time scale, the image diagnosis based on image intensifiers or intensified charge-coupled devices (iCCDs) is widely used in this time scale. The characteristics of streamer channels and leader channels can be analyzed.[4] The statistical characteristics of the discharge phenomenon are obvious in longer time scales, even when there is a strong uncertainty of a single discharge.[5,6] Therefore, the imaging diagnosis of the discharge at long time scales have unique advantages, like the determination of the structure or uniformity of the discharge.[7]

The essence of discharge is the ionization and movement of the charged particles under a strong electric field and is closely related to the distribution of the electric field. The electric field is a time-varying electric field under AC voltage. There are new phenomena and characteristics of discharges which need to be studied. The discharge phenomena usually show a strong correlation with the voltage phase. Particularly, there are disparate characteristics of the discharge phenomenon on the different polarities of the voltage.[8] Under this circumstance, the different discharge patterns of different voltage phases cannot be identified via long-term exposure imaging; the statistical characteristics of the discharge cannot be clarified via nanosecond exposure imaging as well. Therefore, in this NOTE, we propose a phase synchronization photography method for the AC discharge and the discharge image in the specified phase window can be obtained.

The key part of this photography method is a motor-driven photography mask, as shown in Fig. 1.

For phase synchronization photography, the rotating frequency of the photography mask needs to be consistent with the frequency of the discharge power supply. Due to the slippage of the asynchronous motor, the rotating speed of the rotor is always lower than the rotating speed of the electromagnetic field, so the synchronous motor should be selected in this photography method. The synchronous motors are often used in power systems as large-scale electric generators with a large volume, so they are not suitable for the applications described in this NOTE. In order to obtain a small-size synchronous motor, we transform a shaded-pole motor into a permanent-magnet synchronous motor with the advantage of the simple structure and the small volume. Replacing the cast aluminum rotor with skewed slots of the shaded-pole motor to the permanent-magnet rotor as shown in Fig. 2, we get a permanent-magnet synchronous motor. The permanent-magnet rotor consists of a nylon skeleton and two cylindrical neodymium-iron-boron magnets with an orderly arrangement. Due to the characteristics of the synchronous motor, its rotation speed is accurately stabilized at the power supply frequency after the rotation is synchronized with the discharge power supply.

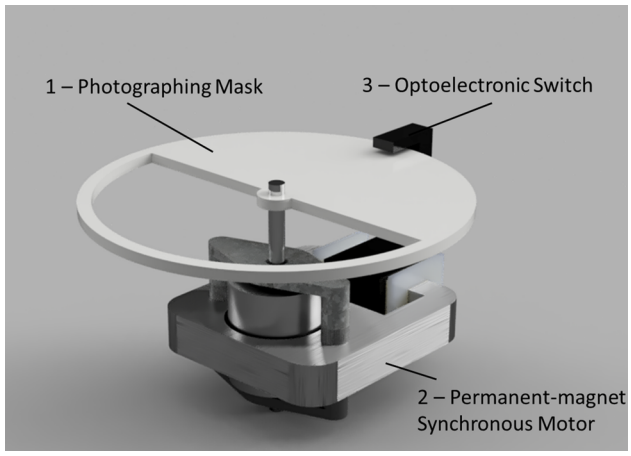

FIG. 1. The photography mask (1) is driven by a permanent-magnet synchronous motor (2) and noted that the photography phase is 180°, corresponding to the central angle of the mask.

[a)]Electronic addresses: z_c_wu@163.com; hvzhang@mail.xjtu.edu.cn; jingtanma@126.com; and plein@163.com.

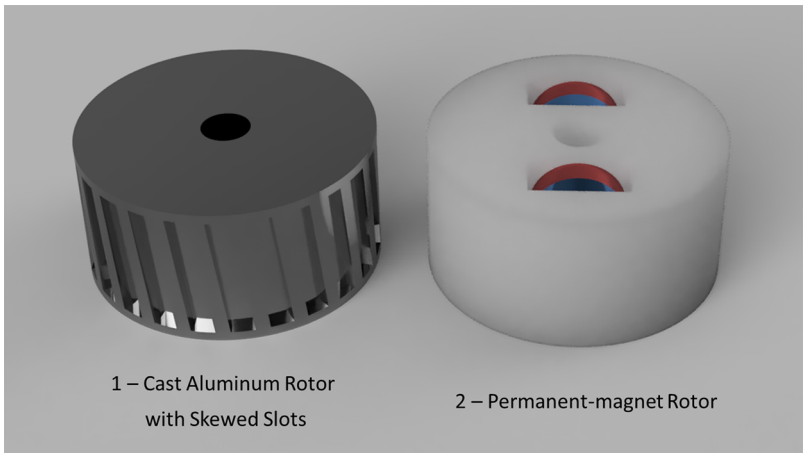

FIG. 2. The permanent-magnet rotor is used to replace the cast aluminum rotor with skewed slots, which is installed in the shaded-pole motor previously.

The photography mask is made of an opaque material with light weight. The sum of the central angle of the photography mask Ω_1 and the desired phase angle of the discharge photography Ω_2 should be equal to a round angle as shown in (1). We set an optoelectronic switch at the outer edge of the mask, in order to clarify the correspondence between the angle of the mask and the voltage phase,

$$\Omega_1 + \Omega_2 = 2\pi. \quad (1)$$

A general camera can be used to record the discharge image behind the photography region of the mask. After the permanent-magnet synchronous motor is synchronized with the discharge power supply, the photography mask cyclically blocks the photography area to record the discharge image in the specified phase window. There are two ways to adjust the phase difference between the photography mask and the discharge power supply. The first method adjusts the relative angle between the motor shaft and the photography mask. Another method is swapping the power cable of the motor to reverse the photography phase window.

The following shows two discharge images taken by the method described in this NOTE: One is the corona discharge in SF_6 and the other is the corona discharge of a floating particle along the air/epoxy surface. The central angle of the photography mask is set to 180° for photographing the discharge images of positive and negative half-cycles. The frequency of the discharge power supply is 50 Hz. The following images are all taken by a NIKON D800 with an exposure time of 2.5 s and a photosensitivity of ISO-6400.

The first example is the corona discharge in SF_6. The gas-insulated metal-enclosed switchgear is filled with SF_6 as an insulating medium. A partial discharge measurement method is used as a general method for gas injection system (GIS) condition monitoring and the phase-resolved partial discharge pattern, which is a typical tool for discharge identification. Yet, engineers are often confused about the interpretation of a

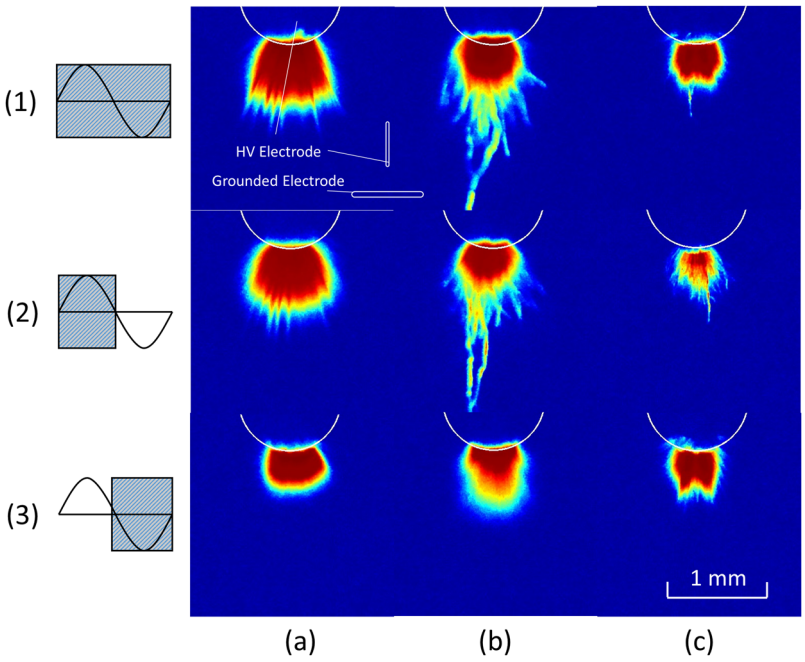

FIG. 3. The corona discharge in SF_6, imaging with and without phase synchronization method. Column label: (a) P = 0.1 MPa and U = 59 kV rms; (b) P = 0.2 MPa and U = 68 kV rms; (c) P = 0.3 MPa and U = 70 kV rms. Row label: (1) without phase synchronization method; (2) phase window = 0°–180°; (3) phase window = 180°–360°.

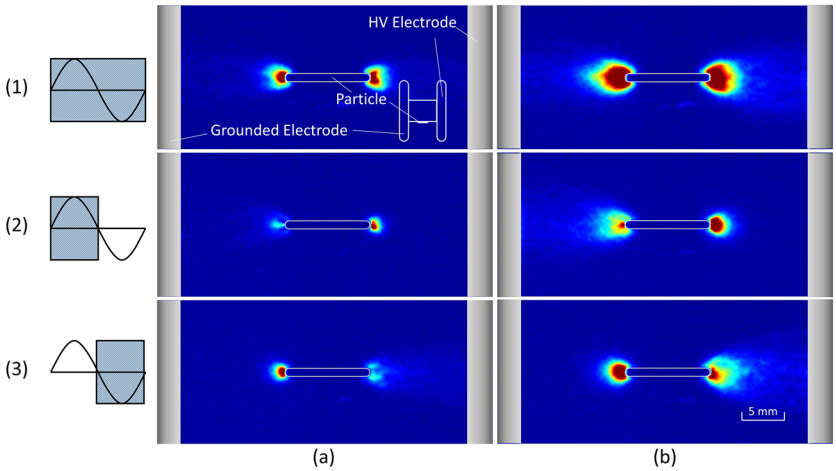

FIG. 4. The corona discharge of a floating particle along the air/epoxy surface, imaging with and without the phase synchronization method. Column label: (a) U = 16 kV rms and (b) U = 19 kV rms. Row label: (1) without the phase synchronization method; (2) phase window = 0°–180°; (3) phase window = 180°–360°.

partial discharge pattern. Therefore, it is necessary to study the discharge processes at the different voltage phases. In this example, the discharge images in SF_6 at the different gas pressures under the different AC voltage are shown as Fig. 3. The electrodes are typical rod-plane electrode systems (rod diameter = 1.0 mm and gap distance = 30 mm). We regard the polarity of the rod electrode as the polarity of the corona discharge. From column (a), the positive and negative streamers have significant differences at 0.1 MPa SF_6. The positive streamer range is larger than the negative streamer range, influenced by the space charge. The negative streamers have been completely blocked by the positive streamer in (a)-(1).[6] From column (b), it can be clarified whether the breakdown leader channel occurs in the positive or negative half-cycle. The positive streamer channel is already converted to the leader channel, stretching into the low-field strength region, while the discharge in the negative half-cycle stays in the negative streamer.[9] From column (c), the leader channel cannot be distinguished clearly in the image without the phase synchronization method, but we can see the lead channels with better spatial resolution in the positive half-cycle. In summary, the phase synchronization method allows researchers to clarify the relationship between the physical discharge processes of the discharge under AC voltage and the voltage phase.

Another example is the corona discharge of a floating particle along the air/epoxy surface. Outdoor insulators are working in a harsh environment. The contamination of various types of contamination will affect the performance of the insulators, such as hydrophobicity. Once conductive particles adhere to the surface of the insulator, both ends of the particles will distort the electric field, and the corona discharge will appear. The corona discharge will degrade the performance of the insulator and may cause insulation failure. In this example, a metallic particle (cylinder particle, length = 10 mm, diameter = 1 mm) is fixed at the vertical center of an epoxy cylinder, which is sandwiched between two plane electrodes, for the purpose of simulating this condition. The discharge images in air under the different AC voltage are shown as Fig. 4. Due to the symmetry of the electrode system, the discharges seem like symmetrical in the discharge images without the phase synchronization method as shown in row (1). Taking advantage of the method mentioned in this NOTE, the different discharge forms can be distinguished clearly at the different ends of the particle as shown in row (2) and (3).[10] The positive streamer discharge still has a wider range, which is consistent with the corona discharge in SF_6. And the range of the negative streamer discharge is much smaller than that of the positive one. In addition, the discharge polarity at one end of the particle and the polarity of the plane electrode close to this end are opposite. Therefore, this discharge photography method is useful for understanding complex discharge processes, such as the combined discharge of the corona discharge and floating discharge in this example.

In conclusion, we presented a phase synchronization photography method for the AC discharge. The photography system consists of a photography mask driven by a permanent-magnet synchronous motor. After the permanent-magnet synchronous motor is synchronized with the discharge power supply, the photography mask cyclically blocks the photography area to record the discharge image in the specified phase window. Some examples of discharge photographed by this method, including the corona discharge in SF_6 and the corona discharge along the air/epoxy surface, demonstrate the feasibility of this method. This method provides an effective tool for discharge physics researchers.

[1] T. H. Thang, Y. Baba, N. Nagaoka *et al.*, IEEE Trans. Electromagn. Compat. **54**(3), 585–593 (2012).
[2] S. Meijier, E. Gulski, and J. J. Smit, IEEE Dielectr. Electr. Insul. **5**(6), 830–842 (1998).
[3] J. R. Roth, *Industrial Plasma Engineering* (Institute of Physics Publishing, Philadelphia, 2001).
[4] H. Luo, Z. Liang, B. Lv, X. Wang, Z. Guan, and L. Wang, Appl. Phys. Lett. **91**, 221504 (2007).
[5] P. Osmokrovic, M. Vujisic, K. Stankovic, A. Vasic, and B. Loncar, Plasma Sources Sci. Technol. **16**, 643–655 (2007).
[6] M. Pejovic, M. Pejovic, and K. Stankovic, Jpn. J. Appl. Phys., Part 1 **50**, 086001 (2011).
[7] I. Radu, R. Bartnikas, G. Czeremuszkin, and M. R. Wertheimer, IEEE Trans. Plasma Sci. **31**(3), 411–421 (2003).
[8] L. Loeb, *Electrical Coronas: Their Basic Physical Mechanisms* (University of California Press, Oakland, 1965).
[9] M. Seeger, L. Niemeyer, and M. Bujotzek, J. Phys. D: Appl. Phys. **41**, 185204 (2008).
[10] N. Hayakawa, K. Hatta, S. Okabe, and H. Okubo, IEEE Trans. Dielectr. Electr. Insul. **13**(4), 842–849 (2006).